Published in final edited form as:
J Am Chem Soc. 2012 May 9; 134(18): 7995–7999. doi:10.1021/ja302588v.

Pharmacokinetics of Py-Im Polyamides Depend on Architecture: Cyclic versus Linear

Jevgenij A. Raskatov[†], **Amanda E. Hargrove**[†], **Alex Y. So**[‡], and **Peter B. Dervan**[†,*]

[†]Division of Chemistry and Chemical Engineering, California Institute of Technology, Pasadena, CA 91125

[‡]Department of Biology, California Institute of Technology, Pasadena, CA 91125

Abstract

The pharmacokinetic properties of three pyrrole-imidazole polyamides of similar size and Py-Im content but different shape were studied in mouse. Remarkably, hairpin and cyclic oligomers programmed for the same DNA sequence 5'-WGGWWW-3' displayed distinct pharmacokinetic properties. Furthermore, the hairpin **1** and cycle **2** exhibited vastly different animal toxicities. These data provide a foundation for design of DNA binding Py-Im polyamides to be tested *in vivo*.

Keywords

Mouse; Pharmacokinetics; Toxicity; DNA binding; Py-Im polyamide

INTRODUCTION

Aberrant regulation of gene expression can result in a diseased state such as autoimmunity,[1–4] or cancer.[5,6] The ability to alter transcriptional profiles in a temporal fashion with small molecules could therefore possess value in the development of novel therapeutic strategies. Pyrroleimidazole (Py-Im) polyamides represent a class of programmable DNA minor groove binders with high affinities and specificities.[7–10] While their applicability to modulate gene expression in cell culture has been studied,[11–17] it is important to transition Py-Im polyamides to *in vivo* experiments. Although there are several examples to this end,[18,19] baseline understanding of *in vivo* properties must be provided before the viability of Py-Im polyamides as modulators for specific disease models can be investigated. We have shown previously that hairpin and cycle Py-Im polyamides can be constructed which bind the same sequence of DNA in the minor groove. As we progress from chemistry to biology, the question arises whether molecules of similar size and similar function but different shape have different properties regarding trafficking in a living mouse.

Here we report the impact of structural modifications on mouse pharmacokinetics of the Py-Im polyamides **1–3** (Fig. 1), employing either the intraperitoneal (IP) or the subcutaneous

[*]**Corresponding Author** To whom correspondence should be addressed: dervan@caltech.edu.
Present Addresses
† Division of Chemistry and Chemical Engineering, California Institute of Technology, Pasadena, CA 91125
‡ Department of Biology, California Institute of Technology, Pasadena, CA 91125

ASSOCIATED CONTENT

Supporting Information. Schematic representation of key synthetic steps and intermediates, HPLC traces of the compounds **1–4**, calibration curve of the analytical HPLC and reproducibility of injection analysis. This material is available free of charge via the Internet at http://pubs.acs.org.

(SC) injection route. Mouse toxicity data associated with the hairpin **1** and cycle **2** are presented. The interest in the polyamides **1–3**, all targeting the genomic sequence 5'-WGGWWW-3', stems from our recent investigation that showed the utility of **1** to modulate NF-κB dependent gene expression in cell culture.[16]

RESULTS

Py-Im polyamides were synthesized following established protocols (Fig. S1). The initial set of in *vivo* experiments compared the plasma levels of the Py-Im polyamides **1–3** as observed 1.5 h following an IP injection (120 nmol / animal; Fig. 2). The concentration of hairpin **1** amounted to 13.8 μM, corresponding to 23 % of the injected compound, if a blood volume of 2 mL per animal is assumed. The plasma levels of cycle **2** were found to be significantly lower with 3.9 μM (6.5 % of injected compound). Most surprisingly, the dication cycle **3**, which is closely related to monocation **2**, was only observed at about 0.7 μM in plasma, which would correspond to 1.2 % of the injected compound. The levels of 3 are approximated because the concentration was close to the detection limit of the HPLC instrument. Control extractions from serum yielded extraction efficiencies of 100 (±4) % (1), 84 (±2) % (2) and 58 (±3) % (3). This implies slightly higher blood levels of 2 (4.6 μM) and 3 (ca. 1.2 μM).

We followed up with a more extensive pharmacokinetic analysis of the Py-Im polyamides **1** and **2** (Fig. 3) that displayed favorable accumulation in plasma at 1.5 h. Injection of **1** by the IP route with subsequent blood withdrawals at different time points showed a rapid build-up of the compound in plasma. The maximum of 14.8 μM was observed at 1 h post injection, followed by a fast decline and a complete disappearance of the compound from circulation within 24 h. Subcutaneous (SC) injection resulted in a slower elimination of the compound and a somewhat more shallow curve overall (10.4 μM peak at 3 h post injection; Fig. 3A), although again, no compound was detected 24 h post injection.

The circulation profile of cycle **2** was strikingly different (Fig. 3B). The initial plasma levels, measured 1.5 h post injection, were substantially lower than those observed with hairpin **1**. Most interestingly, the compound remained in the bloodstream at micromolar levels throughout the experiment and was still readily detectable 48 h post injection (0.8 μM following IP and 2.1 μM following SC injection). An attempt was made to obtain the 72 h time point; however, acute toxicity to the mice was observed. The animals began losing weight, appeared lethargic and had to be euthanized for humane purposes.

The adverse reaction of animals to cycle **2** but not hairpin **1** merited further investigation. Animal weight was used as a proxy for body condition with weight loss of over 15 % being considered an endpoint criterion for the mice. The polyamide **1** was studied first (Fig. 4A,B). We found that the compound could be injected by either IP or SC at 120 nmol per animal per injection over the course of two weeks without an adverse reaction (six injections overall). Given the acute toxicity of cycle **2** at 120 nmol per animal, the corresponding prolonged exposure experiments were conducted at a lower dosage. The dosing regimen was scaled in line with dilution factors typically used in our cell culture experiments. Administration of 30 nmol of **2** per animal (IP or SC, see Fig. 4C,D) alleviated the symptoms of acute toxicity, i.e. the mice did not appear lethargic and displayed no unwillingness to ambulate when gently touched. However, critical weight loss became observable beginning with day 4. The animals typically reached their endpoints within a week. This is a profound difference to the hairpin polyamide **1**, which was tolerated at a total of 720 nmol over two weeks without any obvious health impediment to the animals.

DISCUSSION

The hairpin Py-Im polyamide **1** was detectable in plasma at peak concentrations of 14.8 μM and 10.4 μM, following IP and SC injection, respectively. The drop in circulating levels of **1** was more rapid following IP than SC injection, but the polyamide was not detectable after 24 h for both routes (Fig. 3A). These findings can be compared to recent studies of rat pharmacokinetics of the hairpin polyamides Ac-Im-Py-Py-γ-Im-Py-Py-β-Dp (compound 1035) and Ac-Py-Py-β-Py-Im-Py-γ-Py-Py-Py-β-Im-Py-β-Dp (compound 1666) following intravenous (IV) injection.[19,20] Matsumoto and co-workers reported rat plasma levels drop to low percent over 3 h for both Py-Im polyamides. Because the molecules were administered intravenously, there was no plasma level buildup characteristic for IP and SC injections as we observed for **1**. The highest plasma levels of both 1035 and 1666 were determined at the earliest measured time points. Overall the clearance rates of 1035 and 1666 from rat plasma appear higher than what we observed for the hairpin **1**. However, because of difference in animal model (mouse *vs* rat), administration route (IP and SC *vs* IV) and compound architecture, only qualitative comparisons can be made.

The cyclic polyamides **2** and **3**, which differ in charge, exhibited lower plasma levels than the hairpin polyamide **1**, suggesting that molecular shape is a determinant for the pharmacokinetics of Py-Im polyamides. The macrocycles **2** and **3** are less flexible than the hairpin **1**. Along with the charge difference between **2** and **3**, this could result in altered interstitial tissue penetration rates, clearance rates by the reticuloendothelial system and adsorption propensities onto plasma proteins or the vascular endothelium. The prolonged circulation times of the monocationic macrocycle **2**, as opposed to the hairpin **1**, are in agreement with the recent findings made by Nasongkla *et al* who compared the pharmacokinetic profiles of linear and cyclic polymers with unrelated composition.[21] The phenomenon was ascribed to the differential ability of the molecules to traverse kidney nanopores. The difference in overall charge is a possible origin of the contrast between the pharmacokinetic properties of the macrocycles **2** (monocationic) and **3** (dicationic). Charge effects on pharmacokinetics and bioavailability of oligomers and proteins with otherwise similar steric requirements have been previously reported.[22–24]

The sharp contrast in mouse toxicity of the hairpin **1** and the cycle **2** is potentially rooted in the distinct blood circulation profiles of the two molecules. However, other contributing forces, such as the existence of toxic metabolites of cycle **2** but not hairpin **1**, cannot be ruled out at this time.

CONCLUSIONS

In this investigation we compared the pharmacokinetic properties of the Py-Im polyamides **1–3**. While possessing an identical heterocyclic eight-ring framework, the chemical variations among these compounds were sufficient to give rise to three distinct pharmacokinetic profiles in a mouse model. The hairpin polyamide **1** had a rapid bloodstream accumulation / excretion profile, while cycle **2** could circulate in animals for at least 48 h. The dicationic macrocycle **3** exhibited substantially lower plasma level than its monocationic analog **2**. A stark contrast was observed between the toxic profiles of **1** and **2**: while hairpin **1** was tolerated well by the animals, the injection of cycle **2** proved lethal. We have shown previously that hairpin **1** is capable of modulating NF-κB dependent gene transcription in cell culture. This study sets the stage for comparison of gene expression profiles from cell culture experiments with tumor xenografts in animals. These results will be reported in due course.

EXPERIMENTAL SECTION

Polyamide synthesis

Kaiser oxime resin (LL, 200–400 mesh), benzotriazole-1-yl-oxytrispyrrolidinophosphonium hexafluorophosphate (Py-BOP), and Boc-4-aminobutanoic acid were purchased from Novabiochem. All other reagents were purchased from Sigma-Aldrich. Preparative HPLC purification was performed on an Agilent 1200 Series instrument equipped with a Phenomenex Gemini preparative column (250 × 21.2 mm, 5μm) with the mobile phase consisting of a gradient of acetonitrile (MeCN) in 0.1% CF_3CO_2H (aqueous). Analytical HPLC analysis was conducted on a Beckman Gold instrument equipped with a Phenomenex Gemini analytical column (250 × 4.6 mm, 5μm), a diode array detector, and the mobile phase consisting of a gradient of MeCN in 0.1% CF_3CO_2H (aqueous). Polyamide concentrations were measured by UV analysis on a Hewlett-Packard model 8453 diode array spectrophotometer in distilled and deionized water (ddH_2O) using a molar extinction coefficient (ε) of 69,500 $M^{-1}cm^{-1}$ at 310 nm. Matrix-assisted, LASER desorption/ionization time-of-flight (MALDI-TOF) mass spectrometry was performed on an Applied Biosystems Voyager DE-Pro spectrometer using α-cyano-4-hydroxycinnamic acid as the matrix.

ImImPyPy-(*R*)$^{\alpha\text{-H2N}}$γ-PyPyPyPy-(+)-IPA, **1**. Compound **1** was synthesized using previously described methods. In brief, the Py-Im sequence was built on Kaiser oxime resin and subsequently cleaved with 3,3'-diamino-N-methyldipropylamine.[16,25] The crude compound was precipitated with Et_2O, dried and subjected to isophthalic acid conjugation using standard PyBOP coupling conditions. The resultant mixture was deprotected (99 % TFA, 1 % Et_3SiH, 10 min) and purified by preparative reversephase HPLC, affording the final product in 16 % overall yield (20 μmol). Compound purity was confirmed by analytical HPLC (Fig. S3) and MALDI and was in agreement with previously published data.[16]

cyclo-(-ImImPyPy-(*R*)$^{\beta\text{-H2N}}$γ-PyPyPyPy-γ-), **2**. Compound **2** was synthesized using previously described methods. In brief, the Py-Im sequence was built on Kaiser oxime resin and subsequently cleaved with DBU to give the precursor compound NH_2-γ-ImImPyPy-(*R*)$^{\beta\text{-NHCBz}}$γ-PyPyPyPy-OH.[16,25] Following purification by preparative HPLC, the precursor was subjected to cyclization conditions using diphenyl phosphoryl azide and *N,N*-diisopropylethylamine in DMF.[26] The DMF was then removed by rotary evaporation, and the residue was repeatedly precipitated from cold diethyl ether to remove all traces of base. The isolated residue was submitted to deprotection conditions using a mixture of trifluoroacetic acid and trifluoromethanesulfonic acid,[27] and polyamide **2** was then purified by preparative HPLC (0.7 % overall yield; 2.6 μmol). The key synthetic steps are schematized in Fig. S1. Compound purity was confirmed by analytical HPLC (Fig. S3) and MALDI (calc'd for M+H 1164.5, found 1164.9).

cyclo-(-ImImPyPy-(*R*)$^{\beta\text{-H2N}}$γ-PyPyPyPy-(*R*)$^{\beta\text{-H2N}}$γ-), **3**. Compound **3** was synthesized as above, replacing the final boc-4-aminobutanoic acid (γ) residue with a (*R*)-4-(Boc-amino)-3-(Z-amino)butyric acid residue. Polyamide **3** was purified by preparative HPLC (3.1% yield; 1.7 μmol). The key synthetic steps are schematized in Fig. S1. Compound purity was confirmed by analytical HPLC (Fig. S3) and MALDI (calc'd for M+H 1179.5, found o1179.9).

Animal experiments: General mouse handling

All experiments were performed in C57/BL6 mice between 8 and 12 weeks of age. The animals were obtained through the Jackson Laboratory. All compounds were injected as 4:1 PBS/DMSO solutions at 200 μL per injection (U-100 insulin syringes, UltiCare). No precipitate formation was observable in any of the experiments. Blood was collected by

retro-orbital withdrawal, using heparinized 75MM hematocrit tubes (Drummond). During blood collection the animals were anesthetized with 2–5 % isoflurane. Their breathing frequency was monitored and not allowed to drop below 1 s^{-1}, adjusting the isoflurane levels accordingly. When the animals reached their endpoints, they were euthanized by asphyxiation in a CO_2 chamber.

Animal experiments: Pharmacokinetic analyses

Experiments were conducted in groups of four C57/BL6 mice. Plasma was obtained by centrifugation of the collected blood at $6 \times 10^3 \times g$ for 5 min. The supernatant was isolated, typically yielding approximately 50 μL mouse serum. The samples from the four replicate mice were combined at 5 μL / sample, yielding 20 μL combined plasma that was then treated with 40 uL MeOH, vortexed and centrifuged at $1.6 \times 10^4 \times g$ for 5 min. Fifty μL of the supernatant were isolated and combined with one equivalent of the HPLC loading solution (4:1 water/acetonitrile acidified with 0.08 % trifluoroacetic acid). Boc-Py-OMe (**4**, Fig. S2) was employed as an internal standard to ensure the reproducibility of HPLC injections. Analytical HPLC analyses were conducted on a Beckman Gold instrument equipped with a Phenomenex Kinetex C18 analytical column (100 × 4.6 mm, 2.6 μm, 100 Å) and a diode array detector. The mobile phase consisted of a gradient of acetonitrile (MeCN) in 0.1% (v/v) aqueous CF_3CO_2H (5% to 60% MeCN at 2.0 mL/min over 12.5 min). Peaks were detected and integrated at 310 nm absorbance using the Karat32 software. Sample concentrations were determined through interpolation against a standard curve of concentration vs. peak area generated using compound **1** (Fig. S4). Injection reproducibility was below 15 % error for both IP and SC (see Fig. S5 and Table S1 for standard deviations).

Determination of the extraction efficiency from mouse plasma

All experiments were conducted using C57/BL6 mouse plasma (GeneTex). The plasma was freshly centrifuged to remove residual particles prior to use. DMSO stock solutions of polyamides **1–** were made at 1.5 mM concentrations. To an eppendorf tube containing 198 μL mouse plasma 2 μL of a stock solution were added, the mixture vortexed and allowed to incubate for 15 min. Two separate batches of 20 μL were then taken and treated with 40 μL methanol each, followed by vigorous vortexing and centrifugation at 16000 × g for 5 min. From each of the samples 50 μL supernatant were withdrawn and combined, followed by the addition of 80 μL aqueous 0.01 % trifluoroacetic acid and the reference standard in 20 μL acetonitrile. The thus obtained sample was injected onto the analytical HPLC in technical duplicate at 40 μL per injection. To obtain the maximum expected values, the 1.5 mM stock solutions were diluted 1:6 (DMSO) to mimic the dilution coefficient resulting from the plasma workup. Two μL of the resultant DMSO solution were added to 178 μL aqueous 0.01 % trifluoroacetic acid, followed by the reference standard in 20 μL acetonitrile. The sample was then injected onto the analytical HPLC in technical duplicate at 40 μL per injection. Each extraction experiment was conducted in triplicate to obtain averaged values and standard deviations.

Supplementary Material

Refer to Web version on PubMed Central for supplementary material.

Acknowledgments

JAR is grateful to the Alexander von Humboldt foundation for the award of a Feodor Lynen postdoctoral fellowship. AEH thanks the California Tobacco-Related Disease Research Program (19FT-0105) and the NIH (NRSA number 1F32CA156833) for postdoctoral support. AYS acknowledges the NIH for postdoctoral funding (NRSA number 5F32CA139883). We are grateful for support by The Ellison Medical Foundation (AG-SS-2256-09) and the National Institutes of Health (GM051747).

REFERENCES

1. Cohen PL, Eisenberg RA. Annu. Rev. Immunol. 1991; 9:243–269. [PubMed: 1910678]
2. Raman K, Mohan C. Curr. Opin. Immunol. 2003; 15:651–659. [PubMed: 14630199]
3. Vaux DL, Flavell RA. Curr. Opin. Immunol. 2000; 12:719–724. [PubMed: 11102778]
4. Sospedra M, Martin R. Annu. Rev. Immunol. 2005; 23:683–747. [PubMed: 15771584]
5. Jones PA, Baylin SB. Nat. Rev. Genet. 2002; 3:415–428. [PubMed: 12042769]
6. Vogelstein B, Kinzler KW. Nat. Med. 2004; 10:789–799. [PubMed: 15286780]
7. Dervan PB, Edelson BS. Curr. Opin. Struct. Biol. 2003; 13:284–299. [PubMed: 12831879]
8. Hsu CF, Phillips JW, Trauger JW, Farkas ME, Belitsky JM, Heckel A, Olenyuk BZ, Puckett JW, Wang CCC, Dervan PB. Tetrahedron. 2007; 63:6146–6151. [PubMed: 18596841]
9. Kielkopf CL, White S, Szewczyk JW, Turner JM, Baird EE, Dervan PB, Rees DC. Science. 1998; 282:111–115. [PubMed: 9756473]
10. White S, Szewczyk JW, Turner JM, Baird EE, Dervan PB. Nature. 1998; 391:468–471. [PubMed: 9461213]
11. Olenyuk BZ, Zhang GJ, Klco JM, Nickols NG, Kaelin WG, Dervan PB. Proc. Natl. Acad. Sci. USA. 2004; 101:16768–16773. [PubMed: 15556999]
12. Nickols NG, Jacobs CS, Farkas ME, Dervan PB. ACS Chem. Biol. 2007; 2:561–571. [PubMed: 17708671]
13. Nickols NG, Dervan PB. Proc. Natl. Acad. Sci. USA. 2007; 104:10418–10423. [PubMed: 17566103]
14. Muzikar KA, Nickols NG, Dervan PB. Proc. Natl. Acad. Sci. USA. 2009; 106:16598–16603. [PubMed: 19805343]
15. Matsuda H, Fukuda N, Ueno T, Katakawa M, Wang X, Watanabe T, Matsui SI, Aoyama T, Saito K, Bando T, Matsumoto Y, Nagase H, Matsumoto K, Sugiyama H. Kidney Int. 2011; 79:46–56. [PubMed: 20861821]
16. Raskatov JA, Meier JL, Puckett JW, Yang FT, Ramakrishnan P, Dervan PB. Proc. Natl. Acad. Sci. USA. 2012; 109:1023–1028. [PubMed: 22203967]
17. Chenoweth DM, Dervan PB. Proc. Natl. Acad. Sci. USA. 2009; 106:13175–13179. [PubMed: 19666554]
18. Harki DA, Satyamurthy N, Stout DB, Phelps ME, Dervan PB. Proc. Natl. Acad. Sci. USA. 2008:13039–13044. [PubMed: 18753620]
19. Nagashima T, Aoyama T, Yokoe T, Fukasawa A, Fukuda N, Ueno T, Sugiyama H, Nagase H, Matsumoto Y. Biol. Pharm. Bull. 2009; 32:921–927. [PubMed: 19420765]
20. Fukasawa A, Nagashima T, Aoyama T, Fukuda N, Hiroyuki M, Ueno T, Sugiyama H, Nagase H, Matsumoto Y. J. Chromatogr. B. 2007; 859:272–275.
21. Nasongkla N, Chen B, Macaraeg N, Fox ME, Frechet JMJ, Szoka FC. J. Am. Chem. Soc. 2009; 131:3842–3843. [PubMed: 19256497]
22. Rippe B, Haraldsson B. Physiol. Rev. 1994; 74:163–219. [PubMed: 8295933]
23. Gilchrist SA, Parker JC. Microvascular Res. 1985; 30:88–98.
24. Dellian M, Yuan F, Trubetskoy VS, Torchilin VP, Jain RK. Br. J. Cancer. 2000; 82:1513–1518. [PubMed: 10789717]
25. Belitsky JM, Nguyen DH, Wurtz NR, Dervan PB. Bioorg. Med. Chem. 2002; 10:2767–2774. [PubMed: 12057666]
26. Cho J, Parks ME, Dervan PB. Proc. Natl. Acad. Sci. USA. 1995; 92:10389–10392. [PubMed: 7479790]
27. Dose C, Farkas ME, Chenoweth DM, Dervan PB. J. Am. Chem. Soc. 2008; 130:6859–6866. [PubMed: 18459783]

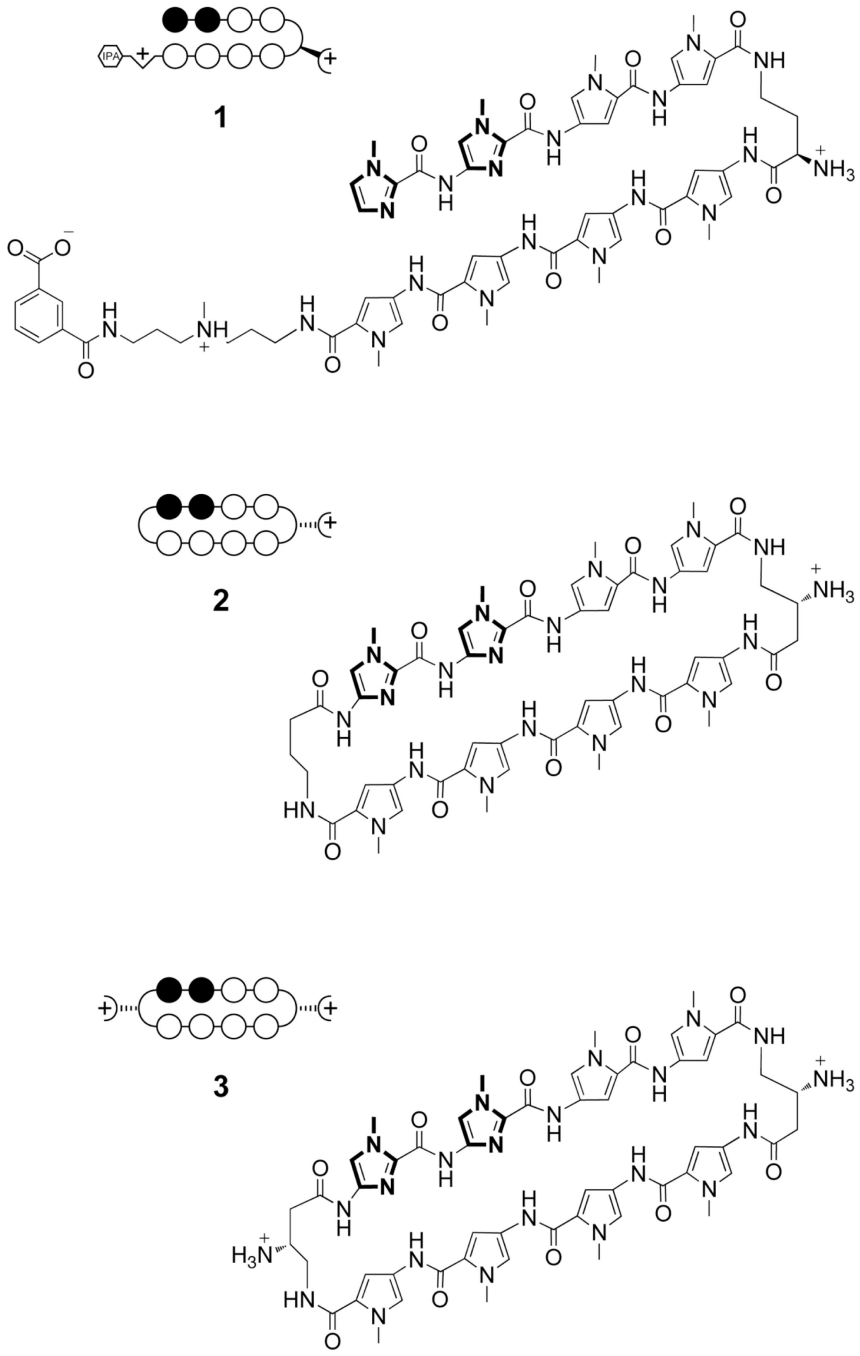

Figure 1.
Chemical structures and circle-stick models of Py-Im polyamides **1**, **2** and **3**. Open circles represent pyrroles and closed – imidazoles. For key synthetic steps see Fig. S1.

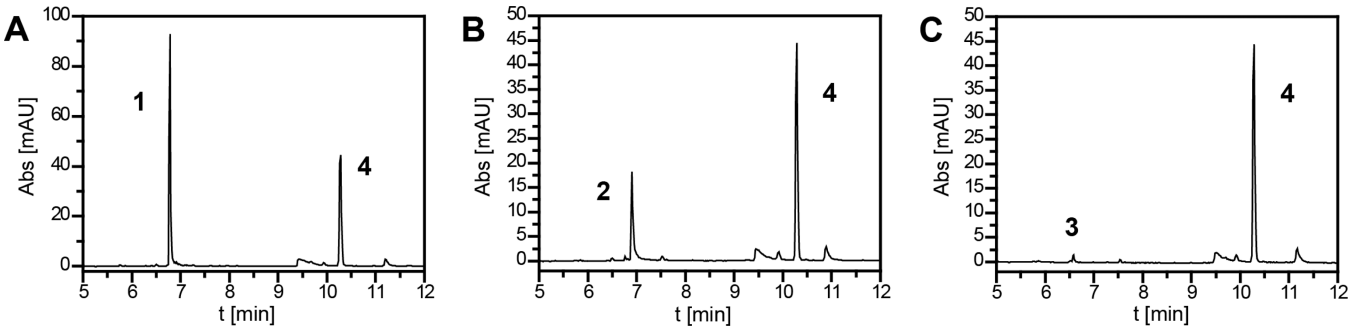

Figure 2.

Plasma levels of the compounds **1–3** (A–C, respectively) measured 1.5 h post intraperitoneal (IP) injection into C57/BL6 mice (120 nmol per animal; 4 animals per group). HPLC traces shown (**4** as internal reference standard, see Fig. S2 for chemical structure).

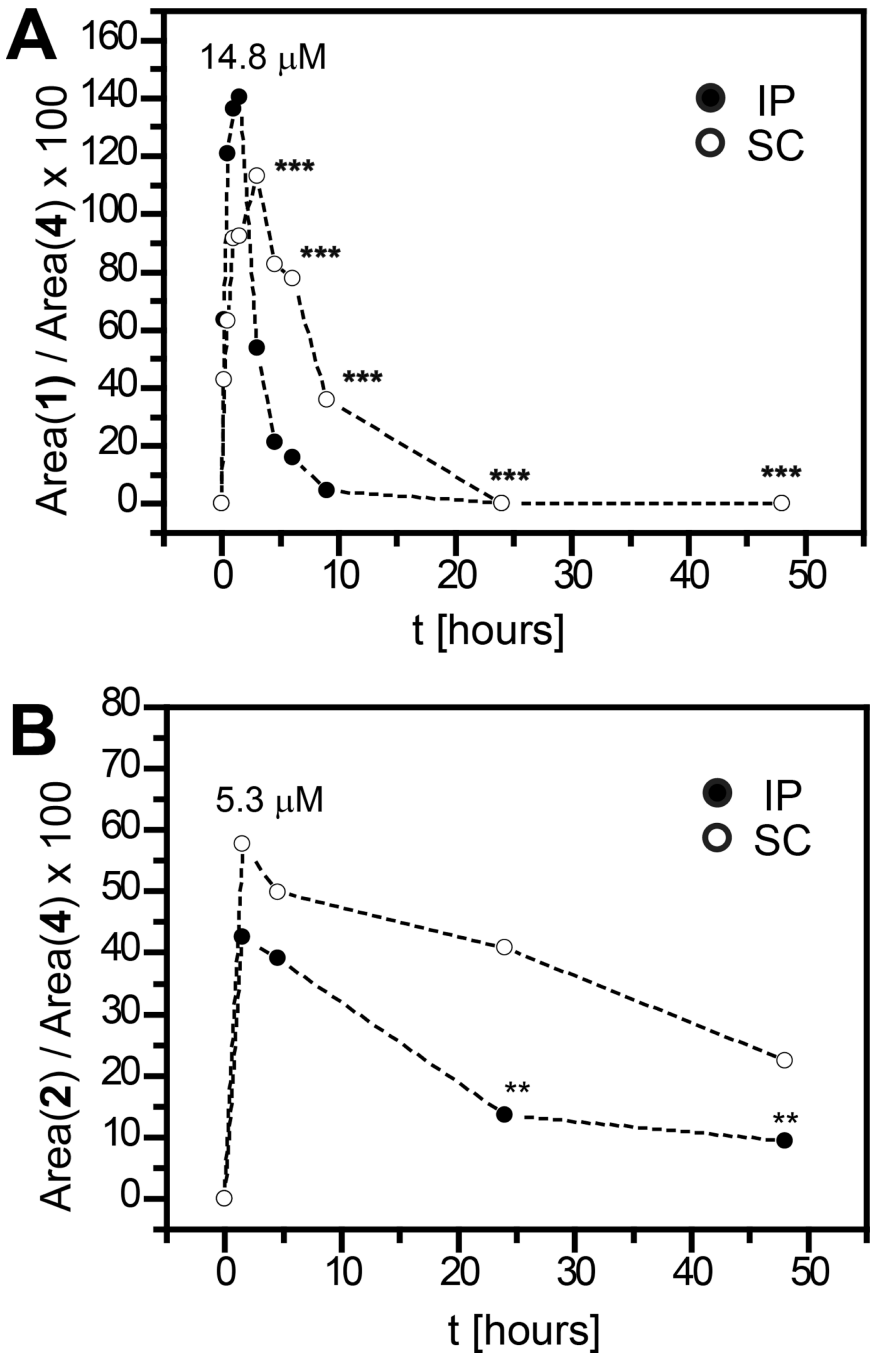

Figure 3.

Plasma levels of the polyamide **1** (A) and **2** (B) as per cent of reference standard **4** (HPLC). IP injections indicated with filled and SC with open circles. All injections at 120 nmol / animal in C57/BL6 wild type mice; 4 animals per group, exceptions indicated as N = 3 (***) and N = 2 (**).

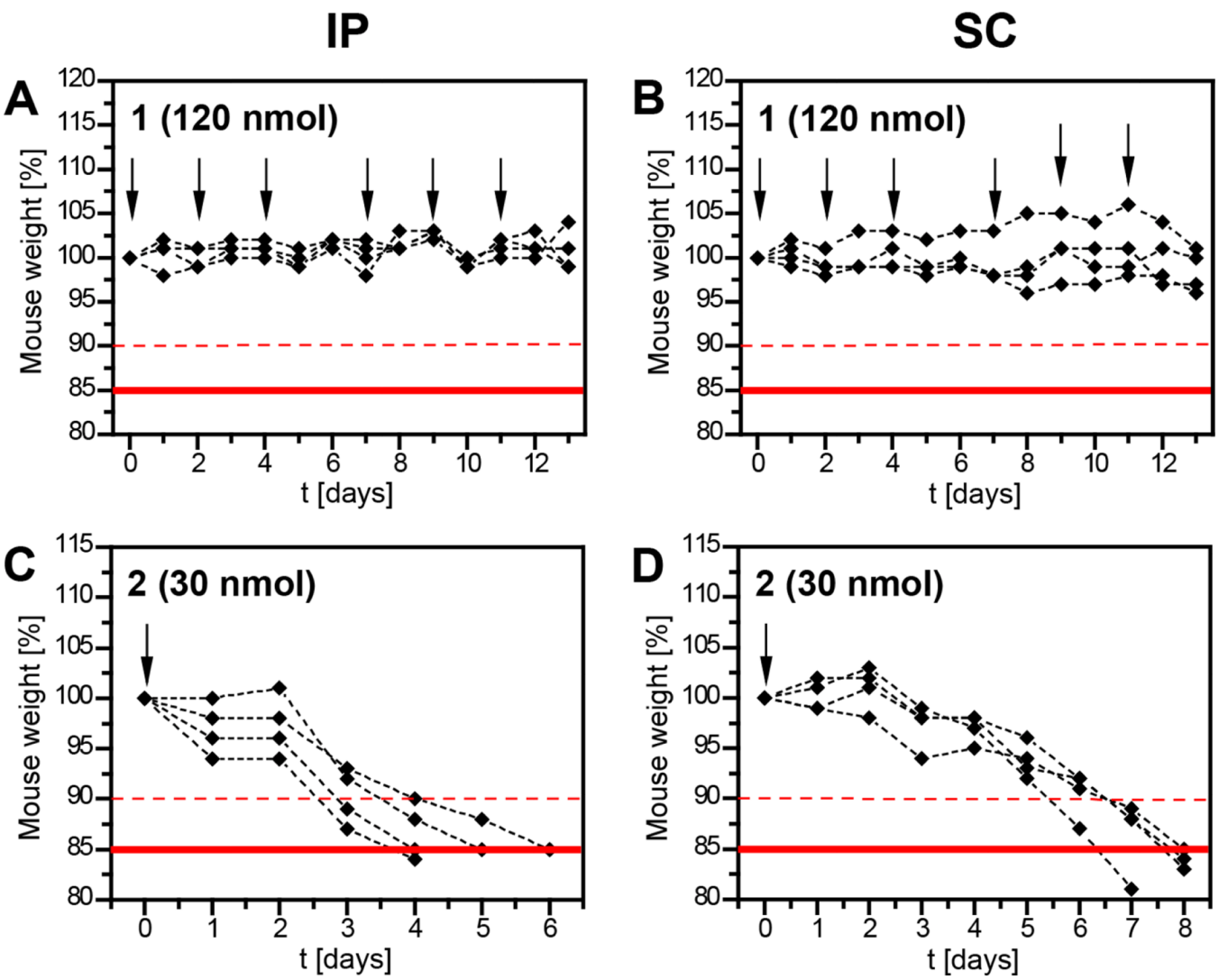

Figure 4.

Mouse weights in response to treatment with polyamide **1** (A,B) and **2** (C,D). Injections at given concentrations are indicated with arrows. All injections were done in C57/BL6 wild type mice, 4 animals per group. Each curve represents the weight of an individual animal.